Adsorption of Fluorescein by Protein Crystals

A. Cvetkovic,[1] M. Zomerdijk,[1] A.J.J. Straathof,[1] R. Krishna,[2] L.A.M. van der Wielen[1]

[1]Department of Biotechnology, Delft University of Technology, Julianalaan 67, 2628 BC Delft, The Netherlands; telephone: 31-15-2782330; fax: 31-15-2782355; e-mail: A.J.J.Straathof@tnw.tudelft.nl
[2]Department of Chemical Engineering, University of Amsterdam, Nieuwe Achtergracht 166, 1018 WV Amsterdam, The Netherlands

Received 16 January 2004; accepted 28 April 2004

Published online 9 August 2004 in Wiley InterScience (www.interscience.wiley.com). DOI: 10.1002/bit.20167

Abstract: Adsorption characteristics of native and cross-linked lysozyme crystals were examined using fluorescein as model adsorbate. The adsorption isotherms exhibited Langmuir or linear behavior. The affinity constant (b_1) and the adsorption capacity (Q_{sat}) for fluorescein were found to depend on the type and concentration of co-solute present in the solution. The dynamics of adsorption isotherm transition from Langmuir to linear showed that affinity of lysozyme for solutes increases in the order 2-(cyclohexylamino)ethanesulphonic acid (CHES), 4-morpholinepropanesulphonic acid (MOPS), acetate, fluorescein. Furthermore, the crystal morphology, the degree of cross-linking of the crystals, and, in particular, solution pH were identified as factors determining fluorescein adsorption by the lysozyme crystals. These factors seem to affect crystal capacity for the solute more than affinity for the solute. Adsorption of fluorescein by cross-linked tetragonal lysozyme crystals was exponentially dependent on the lysozyme net charge calculated from the final solution pH. The 3–5-fold increase in the fluorescein adsorption as a result of cross-linking is presumably due to the increasing hydrophobicity of the lysozyme crystal. © 2004 Wiley Periodicals, Inc.

Keywords: lysozyme crystals; adsorption; distribution; fluorescein; cross-linking

INTRODUCTION

Protein crystals are characterized by their mesoporic morphology, with a porosity content ranging from 25–60% (Matthews, 1968), pore diameters in the range of 0.5–10 nm (Matthews, 1968; Vilenchik et al., 1998), pore volume of 0.9–3.6 mL g^{-1} (Vilenchik et al., 1998), and a total surface area of 800–3,000 m^2 g^{-1} (Morozov et al., 1995; Vilenchik et al., 1998). They are used for studying the mechanisms by which ligands bind to protein molecules and catalyze reactions, and for studying transport processes that might cause differences between the properties of crystalline and dissolved proteins (Rupley, 1969). Cross-linked protein crystals may find a broad range of applications in biocatalysis (Margolin and Navia, 2001; St Clair and Navia, 1992), in medical formulations, in detergents (Margolin and Navia, 2001), in separation processes such as chromatography (Vilenchik et al., 1998), and in biosensors (Morozov and Morozova, 1992).

The wide range of potential applications of protein crystals is a result of the protein crystal's molecular nature and crystal characteristics. For development of any of the protein crystal applications, full understanding of either would be highly beneficial for performing protein engineering and crystal engineering in order to develop improved products. Crystal engineering includes crystallization and crystal stabilization by cross-linking with bifunctional agents, and will affect the specific crystal shape, pore distribution and connectivity, charge distribution, and accessibility of active sites.

In the application of protein crystals, the equilibrium and rate of adsorbate uptake by and release from protein crystals plays a major role. Therefore, adsorption and diffusion are equally important in their influence of the net transport process. Diffusion of solutes in protein crystals has been the subject of several studies (Bishop and Richards, 1968; Botin and Morozov, 1985; Cvetkovic et al., 2004; Granick, 1942; Kachalova et al., 1995; O'Hara et al., 1995; Velev et al., 2000). Some of these studies suggested a high influence of adsorption on transport rates but did not investigate adsorption equilibria separately from diffusion rates (Botin and Morozov, 1985; Velev et al., 2000).

Some isolated adsorption studies exist. Gevorkyan and Morozov (1983) investigated hydration and dehydration of cross-linked lysozyme crystals in air saturated with water vapor and at low humidities found a Langmuir adsorption isotherm. The electrophoretic mobility of NaCl, $NaNO_3$, and NaSCN adsorbed by tetragonal lysozyme crystals from aqueous solutions was highly dependent on solution pH and ionic strength (Lee et al., 2001). There is no reported literature on solute adsorption equilibria for other protein

Correspondence to: A.J.J. Straathof
Contract grant sponsor: Netherlands Foundation for Scientific Research – Chemical Sciences (NWO)

crystals. Thus, understanding of solute adsorption by protein crystals is still in its infancy. The aim of this study is to clarify the influence of several variables on solute adsorption by lysozyme crystals. The variables that will be investigated are solution pH, co-solute type and concentration, and cross-linking.

In the experiments, the type of solute (fluorescein), protein (lysozyme), and solvent (water) were fixed. As mentioned before, understanding of adsorption as well as diffusion of solutes is important for application of protein crystals as a separation material. Therefore, we carried out the present adsorption studies using a model solute (fluorescein) for which diffusion in protein crystals has been studied (Cvetkovic et al., 2004). Chicken egg-white lysozyme was chosen as the model protein because the crystals can be obtained easily and reproducibly, and because the properties and morphologies of these crystals are well known. Lysozyme crystallizes in four different crystal morphologies (Table I). The native crystal's chemical and mechanical stability is very low; therefore, cross-linking with various bifunctional agents is required for most applications.

To be able to compare adsorption equilibria for native and cross-linked crystals, experiments were performed using fluorescein dissolved in the mother liquor of the protein crystallization; otherwise, the native crystals would not be stable. Consequently, the initial aqueous phase composition was different for each crystal morphology. Cross-linked lysozyme crystals, however, are stable and were used to determine the influence of the initial aqueous phase composition on solute uptake. The cross-linked tetragonal lysozyme morphology was used as the base case.

MATERIALS AND METHODS

Crystallization and Cross-Linking of Lysozyme Crystals

Chicken egg-white lysozyme was obtained from Sigma (St. Louis, MO; no. L-6876; 95% purity; M = 14,307 g.mol^{-1}) and was used without further purification. Four different morphologies of lysozyme crystals (Table I) were grown. Triclinic (P_1) and monoclinic ($P2_1$) lysozyme crystals were grown according to the method developed by Steinrauf (1959) in 30 g.L^{-1} and 2 g.L^{-1} aqueous sodium nitrate, respectively, containing 10 g.L^{-1} lysozyme at pH 4.5. Tetragonal lysozyme crystals ($P4_32_12_1$) were grown according to a modification of the procedure described by Feher and Kam (1985). Crystallization solution was prepared from 0.1 mol.L^{-1} sodium acetate buffer with ~6 g.L^{-1} of sodium chloride and 1.5 g.L^{-1} lysozyme at pH 4.5. Orthorhombic lysozyme crystals ($P2_12_12_1$) were grown using the same procedure as for the crystallization of the tetragonal morphology but the pH was adjusted to 10 by the addition of 1 mol.L^{-1} sodium hydroxide.

The above-mentioned solutions were filtered using Schleicher & Schuell (Germany) syringe filters with a cut-off value of 200 nm for sterility and distributed into several glass or plastic vials or tubes. These were closed to allow crystallization by the batch method for 2–14 days. Properties of the crystals are presented in Table I.

Several homo- and heterobifunctional agents have been used for cross-linking of the protein crystals (Margolin and Navia, 2001). Glutaraldehyde was chosen by us because it was the reagent of choice in many applications for fast and dependable protein immobilization (Walt and Agayn, 1994). It is inexpensive, readily available, and easy to use. Unless indicated otherwise, the native and cross-linked forms of a particular crystal morphology originated from the same crystallization solution. One day before the adsorption experiments, one of the tubes was taken apart for cross-linking of the crystals. The mother liquor was decanted up to the top level of the crystals. A 25% glutaraldehyde solution was added until the concentration in the vial was 5% (v/v). After sealing, the mixture was kept unstirred for 20 min and then gently shaken for 40 min. The crystals were filtered using a 0.45 μm membrane filter (Supor – 450, Gelman Laboratory) and then filter-washed with 100 ml of water. The crystals were transferred into tubes filled with 45 ml water and shaken for 30 min. The filtering and shaking procedure was repeated 6–8 times with water, then 6–8 times with 1 mmol.L^{-1} aqueous sodium hydroxide, and finally four times with water to wash out excess sodium hydroxide.

Preparation of Fluorescein Solutions

Sodium fluorescein (Sigma, no. F-6377; M = 376.85 g.mol^{-1}) is a fluorescent dye with a maximum emission at 525 nm if excited by incident light at a wavelength of 490 nm on the solution pH = 9. The value of pK_a, main absorption peak and molar absorptivity are shown in Table II (Sjoback et al., 1995).

Table I. Conditions used for the crystallisation of different lysozyme crystal morphologies.

Crystal morphology	Precipitant	Buffer	pH^{eq}
Tetragonal	1 mol.L^{-1} NaCl	0.1 mol.L^{-1} Na-acetate	4.3–4.7
Orthorhombic	1 mol.L^{-1} NaCl	0.1 mol.L^{-1} Na-acetate	8.8–9.2
Monoclinic	0.16 mol.L^{-1} $NaNO_3$	none	5.3–5.4
Triclinic	0.24 mol.L^{-1} $NaNO_3$	none	4.6–6.8

Table II. Characteristics of fluorescein (Sjoback et al., 1995).

Fluorescein form	pK_a	Main absorption peaks, nm	Molar absorptivities (mol.L^{-1})$^{-1}$.cm^{-1}
Cation	1.25	437	53,000
Neutral	2.08	434	11,000
Monoanion	4.31	472, 453	29,000
Dianion	6.43	490	76,900

Fluorescein degrades within a week when exposed to daylight (Diehl, 1987). To minimize fluorescein degradation, storage of the fluorescein solutions and the experiments were done in a dark room. Fresh solutions were prepared for all experiments. The absorbance of the fluorescein solution, kept in a dark place, was checked and no change was observed for 3 weeks.

To buffer or salt concentration that had been filtered using Schleicher & Schuell syringe filters with a cut-off value of 200 nm, a concentrated solution of sodium fluorescein (2 g.L^{-1}) was added until the desired concentration was reached. A small part of the fluorescein-containing solution was taken apart and used to determine the calibration curve, and the rest was used in adsorption experiments after the density (DMA 48, Anton Paar) and pH had been determined.

In some cases, fluorescein was added to the mother liquor of crystallization instead of the aforementioned buffer or salt solutions. Then the lysozyme content of the resulting solution was also determined by measuring its absorption (Pharmacia, Uppsala, Sweden, Ultrospec III) at 281 nm. The pH of fluorescein-containing mother liquor was adjusted by adding 1 mol.L^{-1} NaOH.

Batch Equilibrium Experiments

The crystals were filtered using 0.45 μm membrane filters (Supor – 200, Gelman Laboratory). Different amounts of the wet (filtered) crystals were placed in vials with 2.00 ml or in tubes with 15 or 45 ml fluorescein solution. For each morphology 10 to 20 vials and/or tubes were prepared for the native and for the cross-linked form. One initial fluorescein concentration ($C_{Fl}^{L,0}$) was used per crystal morphology. The vials were sealed and gently shaken for 7 days at room temperature. After centrifugation, the supernatant was analyzed for fluorescein concentration by spectrophotometry (Pharmacia, Ultrospec III) at the wavelength of the main absorption peak (Hewlett Packard 8453 spectrophotometer).

To determine the time needed to reach equilibrium, two independent sets of experiments were performed. The first set of experiments involved the same scheme as explained before but experiments were performed in 1.5 ml cuvettes for spectrophotometers instead of in 2 ml vials. The contents of the cuvettes were kept unmixed and the fluorescein concentration was measured every 1–5 h until the establishment of equilibrium (constant concentration of fluorescein in the liquid for 24 h). The second set of experiments were dynamic uptake experiments performed in a stirred vessel of 100 ml. Samples of 1.0 ml were taken every 5 min in the beginning of the experiments and then every 2 h, until equilibrium was reached. These samples were centrifuged to separate solution from crystals for the determination of fluorescein concentration. Crystals from the dynamic experiments were filtered under mild conditions and used in the desorption study. These experiments were performed in the same stirred vessel. After 2 weeks of equilibration with water, 90% of fluorescein was desorbed. In additional equilibration with 0.1 mmol L^{-1} NaOH, the rest of the fluorescein was removed from the crystals phase.

Fluorescein adsorption by cross-linked tetragonal crystals from aqueous solutions with fixed initial fluorescein and acetate concentrations and varying chloride concentrations were investigated. The volume ratio of crystals to liquid was kept constant at around 0.0075 (2 ml of solution and 15 μg crystal). The solution pH was adjusted by adding 1 mol.L^{-1} NaOH.

Determination of Crystal Volume (V^{cr})

Following the formalism of Colman and Matthews (1971), a crystal's density (ρ^{cr}) is the sum of densities of its components—namely, protein solid (subscript lys), tightly bound water (subscript w), and free exchangeable solvent (subscript s)—taken in proportion to the fractional volume of each component:

$$\rho^{cr} = \rho_{lys} \cdot \varphi_{lys} + \rho_w \cdot \varphi_w + \rho_s \cdot \varphi_s \tag{1}$$

where ρ_i is the density and φ_i the fractional volume of components. Densities of wet crystals are available in the literature (Table I); the density of the lysozyme is 1,422.4 kg.m^{-3} (Squire and Himmel, 1979); the density of bound water is taken to be 997.5 kg.m^{-3} and the density of free exchangeable solvent is taken to be the same as for the bulk liquid. For every set of experiments the dry mass (m_d) of the crystals was determined. Therefore, part of each batch of filtered crystals was dried for 24 h at 110°C.

Therefore, the crystal volume is:

$$V^{cr} = \frac{m^{cr}}{\rho^{cr}} = \frac{m_d}{\rho^{cr} \cdot (\varphi_w + \varphi_{lys})} \tag{2}$$

where the sum of $\varphi_w + \varphi_{lys}$ is:

$$\varphi_w + \varphi_{lys} = \frac{M_{lys}}{N_A \cdot V_{uc}} \cdot \left(\frac{n_{lys}}{\rho_{lys}} + \frac{n_w}{\rho_w} \right) \tag{3}$$

Here, n_i is the number of component molecules per unit cell, the values of which are given in Table III, and M_{lys} is the molecular mass of lysozyme (14,307 g.mol^{-1}).

The unit cell volume (V_{uc}) is:

$$V_{uc} = a \cdot b \cdot c \cdot \sqrt{1 - cos^2\alpha - cos^2\beta - cos^2\gamma - 2 \cdot cos\alpha \cdot cos\beta \cdot cos\gamma} \tag{4}$$

N_A is Avogadro's number, and *a, b, c* and α, β, γ are the unit cell coordinates and their angles, respectively, the values of which are given in Table III.

Check for Reaction of Fluorescein and Glutaraldehyde

Aqueous solutions of 10 mM fluorescein were prepared containing glutaraldehyde concentrations of 0, 1, 2, 5, 10, 20, 50, and 100 mM. Samples of 1.5 ml of solution

Table III. Characteristics of the lysozyme crystal morphologies.

	PDB name	*a*/nm	*b*/nm	*c*/nm	α	β	γ	n_{lys}	n_w/n_{lys}	ρ^{cr}[a]/kg.m^{-3}	ε[b] (v/v)	φ_{lys}	φ_w	φ_s
Tetragonal	6LYZ	7.91	7.91	3.79	90	90	90	8	101	1242	0.44	0.56[c]	0.10[c]	0.34[c]
Orthorhombic	1AKI	5.906	6.845	3.052	90	90	90	4	78	1304	0.46	0.54	0.08	0.38
Monoclinic	5LYM	2.801	5.25	6.090	90	90.8	90	4	111	1239	0.38	0.62	0.13	0.25
Triclinic	4LZT	2.724	3.187	3.423	88.52	108.53	111.89	1	139	1269	0.36	0.64	0.16	0.20

[a]Steinrauf, 1959.
[b]Calculation according to McRee (1999).
[c]Leung et al., 1999.

were then transferred into sealed cuvettes and their absorption spectrum was determined with a Hewlett Packard 8453 spectrophotometer at consecutive intervals for up to 7 days.

Treatment of Adsorption Data

The adsorption data were analyzed according to the Langmuir model for adsorption isotherm given by:

$$q_{Fl} = \frac{k_1 \cdot Q_{sat} \cdot C_{Fl}^L}{1 + b_1 \cdot C_{Fl}^L} \tag{5}$$

where q_{Fl} is the mol of fluorescein adsorbed per kg of the crystal phase, C_{Fl}^L is the concentration of unadsorbed fluorescein in the bulk liquid at equilibrium, b_1 is affinity constant of the fluorescein for the crystals, and Q_{sat} is a constant indicating the capacity of the crystals for fluorescein. The value of q_{Fl} is determined from a mass balance for the fluorescein considering that no fluorescein degradation or fluorescein glutaraldehyde interaction were detected in the system (see Discussion).

Equation 5 can be rearranged into:

$$\frac{C_{Fl}^L}{q_{Fl}} = \frac{1}{b_1 \cdot Q_{sat}} + \frac{1}{Q_{sat}} \cdot C_{FL}^L \tag{6}$$

A plot of C_{Fl}^L/q_{Fl} vs. C_{Fl}^L should yield a slope of $1/Q_{sat}$ and an intercept of $1/(b_1\ Q_{sat})$. Adsorption data were analyzed using linear regression fits of the data to Eq. 6.

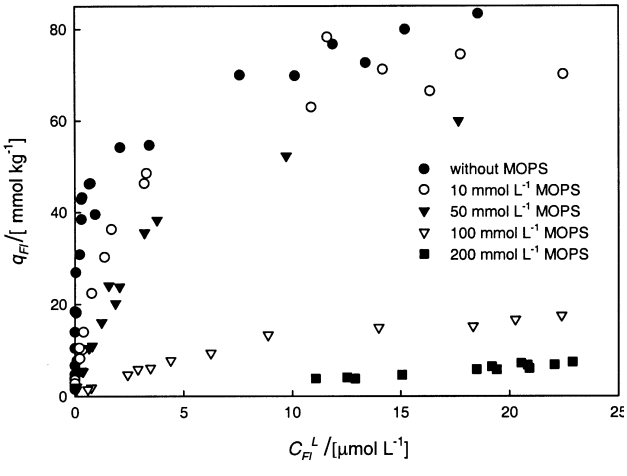

Figure 1. Influence of MOPS presence in the solution on the adsorption of fluorescein by the cross-linked tetragonal lysozyme crystals. Fluorescein initial concentration in the solutions was 25.9 μmol.L^{-1}. For experimental details, see Table IV.

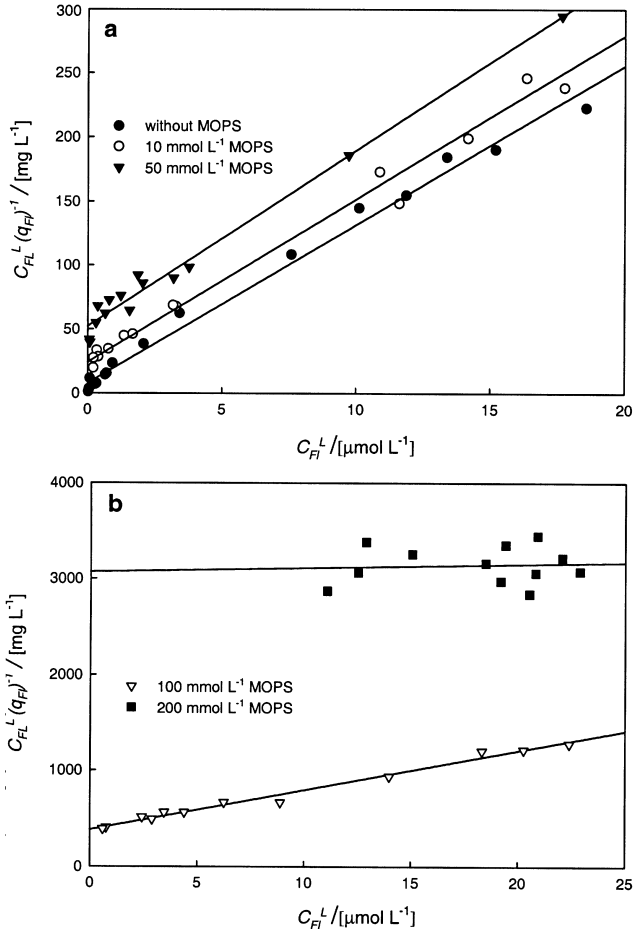

Figure 2. Linear regression fit of the adsorption of fluorescein by cross-linked tetragonal lysozyme crystals from the solutions with constant fluorescein and different MOPS initial concentrations: (**a**) 0, 10, and 50 mmol.L^{-1} and (**b**) 100 and 200 mmol.L^{-1}. Markers are experimental data and lines are fits of Eq. 6.

Table IV. Adsorption of fluorescein from aqueous solution by cross-linked tetragonal lysozyme.

Aqueous solvent	pH^0	pH^{eq}	$b_1/10^4$ L.mol^{-1}	R_L	$Q_{sat}/10^{-2}$ mol.kg^{-1}	Q_{sat}/mol.mol^{-1}*	$K = b_1 Q_{sat}(\rho^{cr})^{-1}$
water	6.71	6.03–6.48	166.2 ± 24.9	0.02 ± 0.00	8.06 ± 0.19	1.15 ± 0.03	134,000 ± 23,600
10 mM MOPS	7.08	6.98–7.08	53.4 ± 7.3	0.07 ± 0.01	7.83 ± 0.21	1.11 ± 0.03	41,700 ± 7000
50 mM MOPS	6.78	6.74–6.82	26.3 ± 0.5	0.13 ± 0.00	7.28 ± 0.28	1.04 ± 0.04	19,100 ± 1100
100 mM MOPS	7.15	7.10–7.15	10.8 ± 0.1	0.26 ± 0.00	2.42 ± 0.09	0.35 ± 0.01	2600 ± 130
200 mM MOPS	7.76	7.76–7.82	—	—	—	—	408 ± 33
10 mM CHES	8.76	7.54–8.72	24.5 ± 1.8	0.14 ± 0.01	3.11 ± 0.14	0.45 ± 0.02	9400 ± 900
10 mM sodium acetate	4.23	4.23–4.34	—	—	—	—	685 ± 14

The initial fluorescein concentration was 25.9 μmol.L^{-1}.
*mol of fluorescein per mol of lysozyme in the crystal.
— could not be calculated using Eq. 6.

A further analysis of the Langmuir equation can be made on the basis of a dimensionless equilibrium parameter, R_L (Hall et al., 1966), also known as the separation factor given by:

$$R_L = \frac{1}{(1 + b_1 \cdot C_{Fl}^{L,0})} \tag{7}$$

It is shown that for favorable adsorption, $0 < R_L < 1$, while $R_L > 1$ represents unfavorable adsorption, and $R_L = 1$ represents linear adsorption, while the adsorption process is irreversible if $R_L = 0$ (Hall et al., 1966).

In the case of a linear adsorption isotherm, Eq. 6 can be simplified:

$$\frac{q_{Fl}}{C_{Fl}^{L}} = b_1 \cdot Q_{sat} = \rho^{cr} \cdot K \tag{8}$$

where K represents the linear distribution coefficient of fluorescein in the system. A plot of C_{Fl}^{L}/q_{Fl} vs. C_{Fl}^{L} would yield a horizontal line with an intercept $1/(b_1\ Q_{sat})$. However, this representation magnifies errors in the determination of q_{Fl} when $C_{Fl}^{L} \approx C_{Fl}^{L,0}$. An alternative approach for data presentation will be employed based on the determination of the distribution coefficient directly from the experimental data using the only variable in the experiment—the crystal volume (V^{cr})—and the mass balance for fluorescein:

$$C_{Fl}^{L,0} \cdot V^{L} = C_{Fl}^{L} \cdot V^{L} + C_{Fl}^{cr} \cdot V^{cr} \tag{9}$$

As the linear distribution coefficient of fluorescein represents $K = C_{Fl}^{cr}/C_{Fl}^{L}$, Eq. 9 can be written as:

$$\frac{C_{Fl}^{L,0}}{C_{Fl}^{L}} = 1 + K \cdot \frac{V^{cr}}{V^{L}} \tag{10}$$

where $C_{Fl}^{L,0}$ and C_{Fl}^{L} are the initial and final concentrations, respectively, of fluorescein in the bulk liquid and V^{L} and V^{cr} are the volumes of bulk liquid and crystal phases, respectively. A plot of $C_{Fl}^{L,0}/C_{Fl}^{L}$ vs. $V^{cr}/\ V^{L}$ should yield a slope of K and an intercept of 1.

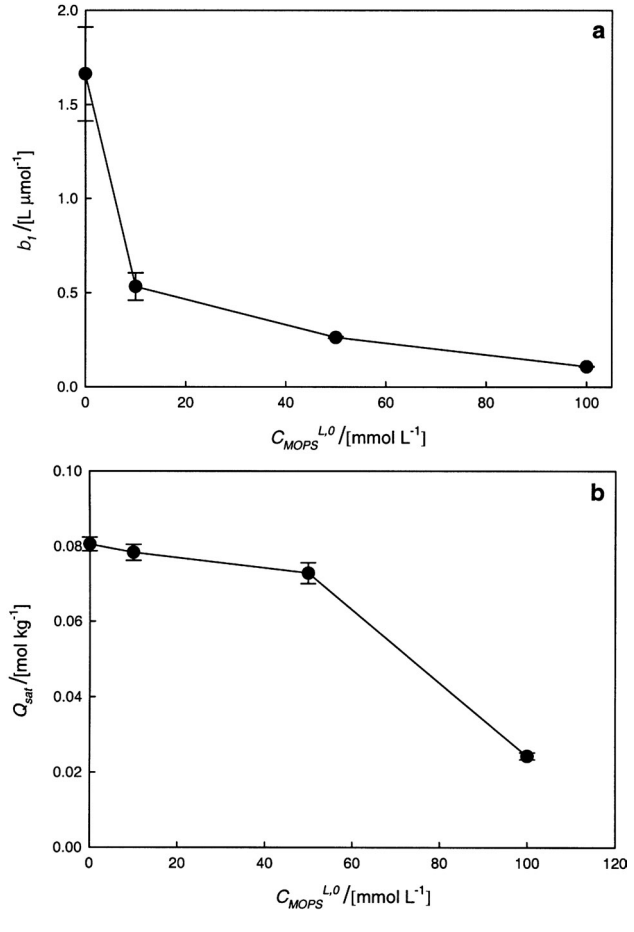

Figure 3. Langmuir coefficients as function of the initial concentration of MOPS in the solutions: (**a**) affinity of the crystal for fluorescein and (**b**) capacity of the crystal for fluorescein. For experimental details see Figure 2 and Table IV.

RESULTS

Cross-Linked Tetragonal Crystals: Influence of MOPS Concentration

During fluorescein adsorption experiments by lysozyme crystals, the pH of the fluorescein solution generally moved in the direction of pH 7–8. This is caused by the buffering effect of the lysozyme, and hence the pH shift is not only dependent on the buffering capacity of the fluorescein solution but also on the amount of crystals. Within a series of experiments, slightly different final pH values were observed.

Typical results of fluorescein adsorption by cross-linked tetragonal crystals from solutions with different initial MOPS concentration are presented in Figure 1. The achievement of equilibria for fluorescein adsorption experiments was confirmed by two independent experimental approaches. Dynamic adsorption experiments performed with cross-linked tetragonal crystal in a stirred system showed no more change in the fluorescein solution's concentration after 1–4 days, depending on the solution pH, whereas in unstirred system this took 3–8 days. During the experiments, there was no swelling of the crystals according to observations by Leica TCS SP confocal microscopy (Cvetkovic et al., 2004). These findings are in agreement with the literature (Morozova et al., 1996).

The adsorption isotherm profiles for fluorescein change with an increase in the initial MOPS concentration from the Type I isotherms (BDDT classification) to almost linear curves for solutions with the two highest MOPS concentrations for experimental conditions used in study (Fig. 1). As a Type I isotherm in BDDT classification is represented by the Langmuir model, the Langmuir model is applied to fit experimental adsorption data (Fig. 2). The good fits indicate that the Langmuir model could be used to describe fluorescein adsorption by lysozyme crystals. Table IV lists the experimental conditions for Figure 1 and the Langmuir parameters b_1 and Q_{sat} calculated using Eq. 6. The values of the Langmuir parameters decreased with increasing MOPS concentrations (Fig. 3). The trend for Q_{sat} (Fig. 3b) points out that they might reach zero above 100 mmol.L^{-1} MOPS.

Cross-Linked Tetragonal Crystals: Influence of Type of Co-Solute

Langmuirian plots of fluorescein adsorption from 10 mmol.L^{-1} solutions of either sodium acetate at pH 4.29, MOPS at pH 7.03, or CHES at pH 8.1 by cross-linked tetragonal crystals are presented in Figure 4. A linear isotherm was established for fluorescein adsorption from the solution with acetate. For the other two solutions classical Langmuir adsorption isotherms were obtained (Fig. 4). Values of the Langmuirian coefficients were approximately two times smaller for the CHES than for the MOPS solution (Table IV). The ratio of the distribution coefficient of the fluorescein between the cross-linked tetragonal crystals and 10 mM solutions of acetate, CHES, and MOPS was 1:14:135, respectively.

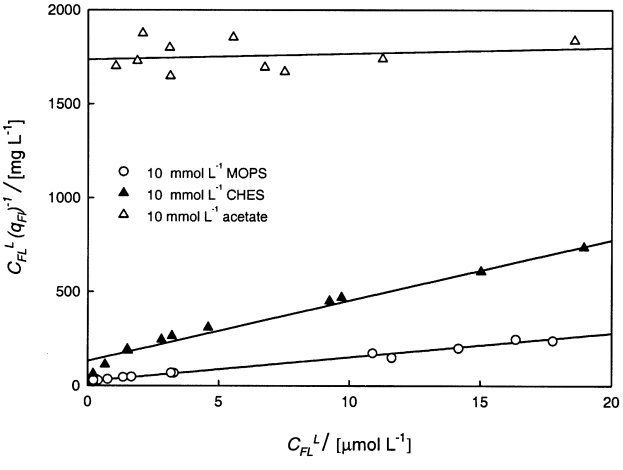

Figure 4. Linear regression fit of the adsorption of fluorescein by cross-linked tetragonal lysozyme crystals from the solutions with constant fluorescein and constant (10 mmol.L^{-1}) concentrations of MOPS (pH^0 = 7.08, pH^{eq} = 6.98–7.08), CHES (pH^0 = 8.76, pH^{eq} = 7.54–8.72) and acetate (pH^0 = 4.23, pH^{eq} = 4.23–4.34).

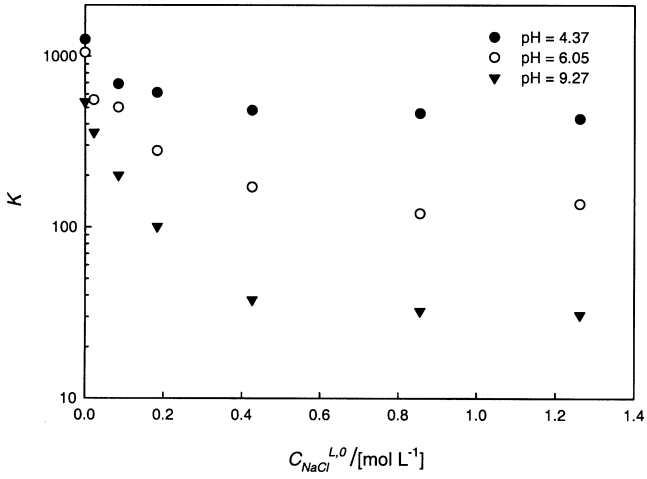

Figure 5. Influence of chloride on the distribution of fluorescein between cross-linked tetragonal lysozyme crystals and solution with constant concentration of acetate and fluorescein (0.1 and 0.0157 mmol.L^{-1}, respectively) at different solution final pH^{eq}.

Cross-linked Tetragonal Crystals: Synchronized Influence of Two Co-Solutes

In the mother liquor of the tetragonal crystal, 0.1 mol.L^{-1} acetate and 1 mol.L^{-1} chloride are present in addition to dissolved lysozyme. This concentration of acetate is 10 times higher than the initial concentration in the experiments presented in Figure 4. For this reason, fluorescein adsorption from the mother liquor by cross-linked tetragonal lysozyme crystals will be linear and can be described using the distribution coefficient of fluorescein as the only

Table V. Distribution of fluorescein between cross-linked tetragonal crystals and bulk aqueous solution with constant acetate concentration of 0.1 mol.L^{-1} and variation of chloride concentration (0 to 1.3 mol.L^{-1}) as presented in Figure 5.

pH^0	pH^{eq}	K[a]
4.30	4.32–4.43	459 ± 11
5.75	5.80–6.15	122 ± 9
9.80	9.00–9.55	33.5 ± 1.7

The initial fluorescein concentration was 15.7 μmol.L^{-1}.
[a]At high NaCl concentration.

model parameter. However, the presence of the chloride in the mother liquor will influence fluorescein distribution between phases and therefore has to be considered as well. Consequently, experiments were performed using constant initial concentrations of fluorescein (0.0157 mmol.L^{-1}) and acetate (0.1 mol.L^{-1}) while varying the chloride concentration in the range from 0–1.3 mol.L^{-1}. The outcome of these experiments is presented in Figure 5 and Table V. A decrease in the distribution coefficient of fluorescein was detected with increasing initial chloride concentration up to 0.5 mol.L^{-1} (Fig. 5). A further increase in the chloride concentration in the solution had no effect on the fluorescein distribution coefficient. The pH determines the value of K at high chloride concentrations. By analogy, at experimental conditions for tetragonal mother liquor (containing about 0.1 mol.L^{-1} acetate and 1 mol.L^{-1} chloride), the distribution of fluorescein between the phases will be independent from the exact chloride and acetate concentrations. This enables us to perform relatively easily an interpretation of experiments with native crystals, where mother liquor has to be used as the solvent. Such experiments are included in the subsequent section.

Influence of Crystal Morphology and Solution pH

Experiments for the system consisting of cross-linked tetragonal crystals (the base case morphology) and fluorescein dissolved in the mother liquor in the initial range of pH 4.51–8.81 are presented in Figure 6 as a function of final (equilibrium) pH. Additionally, the distribution of fluorescein between crystal phase and mother liquor is presented in Figure 7 for the native and cross-linked form of each crystal morphology used in this study, stressing the impact of the cross-linking. In Figures 6 and 7, Eq. 10 fits the experimental data very well, indicating a linear adsorption isotherm. The distribution coefficient of fluorescein decreases with increasing final solution pH (pH^{eq}), if cross-linked tetragonal crystals are used as an adsorbent (Fig. 8 and Table VI). For other native or cross-linked crystal morphologies, not enough data are available to establish such a correlation per crystal type, but the available data seem to be in line with the correlation for the tetragonal morphology. The deviations from the observed tendency might be attributed to differences in the constitutions of their solutions. Hence, there is no indication yet that the distribution of fluorescein between lysozyme crystals and their mother liquor depends on the crystal morphology at these conditions. Considering the data presented in Figure 8, this can be generalized for native crystals too.

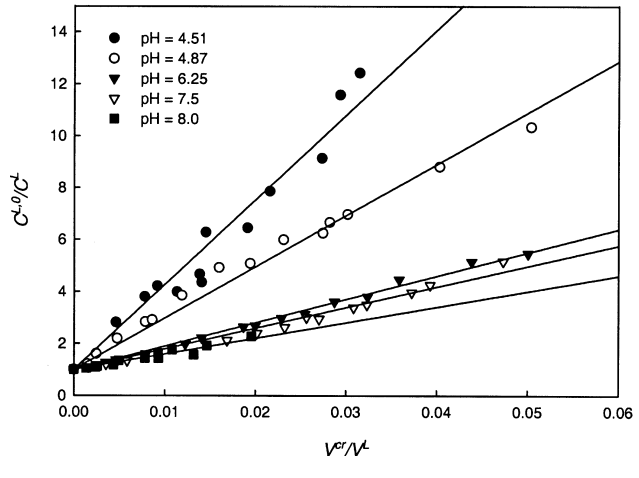

Figure 6. Distribution of fluorescein between mother liquor and cross-linked tetragonal crystals for different solution pH^{eq}. Markers are experimental data and lines are fits of Eq. 10. Experimental details are given in Table VI.

Figure 7 and Table VI show that cross-linking of the protein crystal has a high impact on fluorescein distribution between the phases. Distribution coefficients were 3–5 times higher with cross-linked lysozyme crystals than with native ones.

DISCUSSION

Influence of MOPS Concentration

The choice for the Langmuir model was based on the results presented in Figure 2. However, the validity of two assumptions of the Langmuir model is not immediately clear for protein crystals; namely, that fluorescein adsorption is reversible and confined to a monolayer. The values of R_L indicate favorable and not irreversible adsorption. An observation that >90% of fluorescein was found back in solution upon using 10^{-4} mol.L^{-1} NaOH for desorption from the crystals also supports the assumption of reversibility of fluorescein adsorption. For monolayer or multilayer adsorption, we should consider the total accessible surface of protein and not only the outer crystal surface, according to observations with CLSM (Cvetkovic et al., 2004). Calculations indicate a coverage of 1.4 molecules of fluorescein per molecule of lysozyme if the lowest crystal surface area of 800 g.m^{-2} was assumed for lysozyme crystals (Morozov et al., 1995). This coverage is too low for multilayers, and justifies the use of the Langmuir model for description of the fluorescein diffusion in lysozyme crystals.

The isotherms, despite giving reasonably parallel lines in Figure 2a, did not fit well to Eq. 11, which is a model for competitive binding of fluorescein and MOPS (data not shown):

$$q_{Fl} = \frac{b_1 \cdot Q_{sat} \cdot C^L_{Fl}}{1 + b_1 \cdot C^L_{Fl} + b_2 \cdot C^L_{MOPS}} \tag{11}$$

The interactions will be more complex than simple competition. Noncompetitive binding (Eq. 12), i.e., different sites for different solutes, should lead to steeper slopes in Figure 2 with increasing presence of the co-adsorbate (MOPS), and the lines should all merge at the same (negative) values at

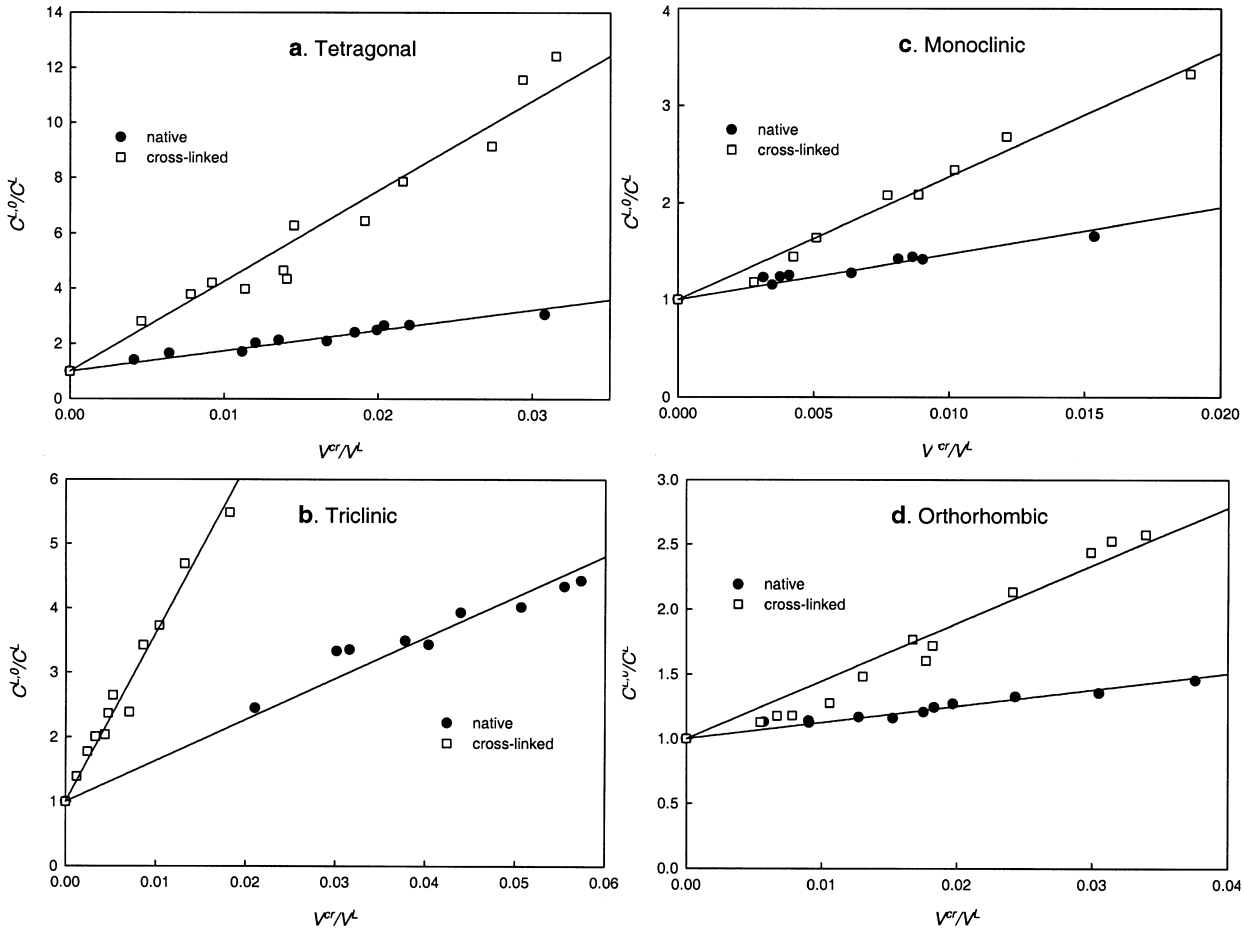

Figure 7. Determination of the fluorescein distribution coefficient between crystal and bulk phase for different crystal morphologies. Markers are experimental data and lines are fits of Eq. 10. Experimental details are given in Table VI.

the x-axis. This was not observed in Figure 2, eliminating noncompetitive binding as the only adsorption mechanism.

$$q_{Fl} = \frac{b_1 \cdot Q_{sat} \cdot C^L_{Fl}}{1 + b_1 \cdot C^L_{Fl} \cdot (1 + b_2 \cdot C^L_{MOPS})} \qquad (12)$$

The sensitivity of fluorescein affinity to crystals (b_1) is high for relatively small concentrations of MOPS in the system and low for high MOPS concentrations (Fig. 3a). This is directly opposite to the behavior observed for a capacity of the crystal to fluorescein (Fig. 3b). An increase in the MOPS concentration up to 50 mmol.L^{-1} did not result in a significant change in the capacity (Fig. 3b). In particular, capacities for two solutions with the lowest MOPS concentration were the same. This observation indicates that there is no competition between fluorescein and MOPS for the adsorption sites of the crystal. A further increase in the MOPS concentration up to 100 mmol.L^{-1} resulted in a decrease of the capacity to one-third of its initial value. This indicates a shift in the adsorption mechanism from noncompetitive to competitive adsorption in the MOPS concentration region from 50 mmol.L^{-1} to 100 mmol.L^{-1}. When the MOPS concentration was 200 mmol.L^{-1} adsorption, only the linear part of Langmuir curve was observed.

A maximum capacity of about 1 mol fluorescein per mol lysozyme (Table IV) suggests that the adsorption is rather specific at a void in the crystal or on a site (perhaps the

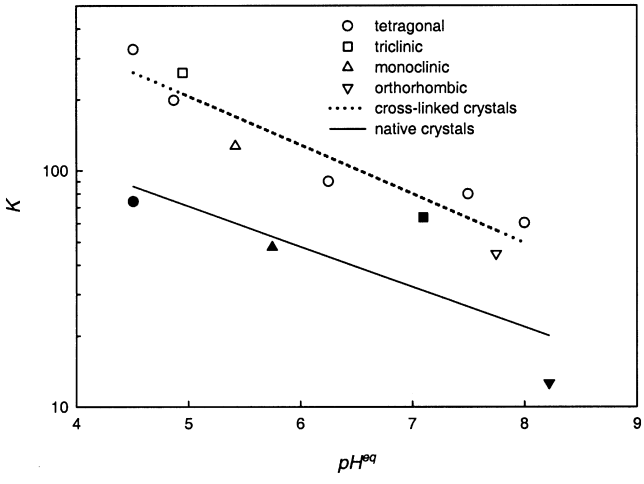

Figure 8. Influence of crystal morphology on fluorescein distribution coefficient. For experimental details see Figures 6 and 7. Full markers are experimental data for native and empty markers for cross-linked lysozyme crystals. The errors in distribution coefficients (K) are shown in Table VI. The lines are given to guide the eye.

Table VI. Distribution of fluorescein between mother liquor and lysozyme crystals at various initial pH values: experimental conditions and results.

Morphology	Cross-linking	$C_{Fl}^{L,0}$, μmol.L^{-1}	pH^0	pH^{eq}	K
Tetragonal	cross-linked	47.6	4.47	4.51	327 ± 11
Tetragonal	cross-linked	25.9	4.70	4.81–4.94	199 ± 12
Tetragonal	cross-linked	25.9	5.80	6.1–6.4	90 ± 1
Tetragonal	cross-linked	25.9	6.80	7.1–7.9	80 ± 2
Tetragonal	cross-linked	25.9	8.80	7.2–8.6	60 ± 3
Triclinic	cross-linked	21.8	4.37	4.6–5.3	260 ± 8
Monoclinic	cross-linked	43.3	5.80	5.3–5.5	127 ± 3
Orthorhombic	cross-linked	24.4	8.81	7.5–8.0	45 ± 2
Tetragonal	native	47.2	4.47	4.51	74 ± 2
Triclinic	native	26.0	6.85	7.0–7.2	63 ± 2
Monoclinic	native	43.3	5.45	5.5–6.0	48 ± 2
Orthorhombic	native	24.4	8.81	8.1–8.5	13 ± 0.4

active site) of the enzyme. However, the information available in the literature does not indicate any binding of compounds like fluorescein by dissolved lysozyme. Note that the model used for binding to sites of enzymes is mathematically equivalent to the Langmuir model for surface adsorption.

Influence of Mother Liquor

The data shown in Table IV suggest that acetate and CHES show a similar effect as MOPS, but already at lower concentrations. Hence, also the salt present in the mother liquor will affect fluorescein adsorption by the crystals. The values of the fluorescein distribution coefficients observed for the mother liquor in Figure 8 and observed for high sodium chloride concentration and 0.1 mol.L^{-1} acetate (Table IV) are consistent. This confirms that for understanding fluorescein adsorption from the mother liquor, adsorption from an aqueous solution of the same pH and salt concentration can be taken.

Solution pH

Distribution of the fluorescein between crystal phase and mother liquor solution depends on the solution pH (Figs. 5, 6, and 8; Tables V, VI). In the pH range used in the experiments, fluorescein exists in the neutral, monoanionic, and dianionic form (see pK_a's in Table II). Conversely, dissolved lysozyme is positively charged with a net charge change from +19 at pH = 2 to 0 at the isoelectric point at pH = 11.2 (Kuehner et al., 1999). Therefore, a maximal uptake was expected around pH 8 when their charge product has the most negative value. Using the distribution coefficients from Tables V and VI, a clear correlation was established only with the lysozyme net charge (Fig. 9), and not with the fluorescein net charge or with the product of their net charges. This correlation holds for tetragonal cross-linked crystals and mother liquor or aqueous solution with the same salt composition as mother liquor, and its origin is not clear.

Internal pH levels of porous polyelectrolyte matrices differ from bulk solution pH due to the Donnan potential (Jansen et al., 1996). Since proteins have positive as well as negative charges, the situation is even more complex than for ion-exchange resins. In the mother liquor solution, the salt concentration exceeds 1.1 mol.L^{-1}. This is sufficient to minimize the difference between external and internal pH and allows us to exclude for most experiments previously discussed the influence of the Donnan potential. However, during uptake of fluorescein from 10 mmol.L^{-1} buffer solutions (MOPS, CHES, and acetate), the Donnan potential may have caused a shift of internal pH. This hypothesis could not be checked due to experimental limitations with respect to measuring the adsorbed amounts of buffering species.

Cross-Linking

As a result of cross-linking, the crystals' porosity might have been decreased, which might have resulted in less uptake of solute than by the native form. Nevertheless, Figures 7 and 8 and Table VI provide the opposite picture, the distribution coefficient of fluorescein for cross-linked crystals was 3–5 times higher than for their native counterparts. Explanations to be considered are:

1. Glutaraldehyde reacts with fluorescein.
2. Initially the cross-linked crystals contain water in the pores, whereas the native crystals contain mother liquor.
3. Cross-linking increases the hydrophobicity of the lysozyme.

1) Glutaraldehyde reacts with lysine residues of lysozyme crystals (Yonath et al., 1977) stabilizing the crystal morphology. In the case that only one of the two

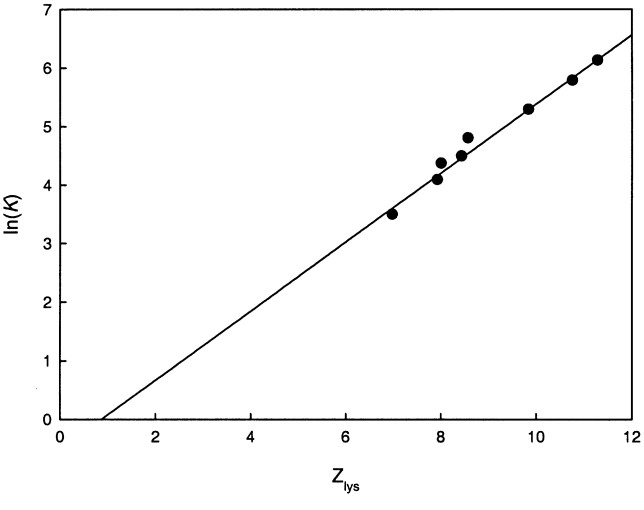

Figure 9. Correlation between charge per lysozyme molecule and distribution of fluorescein between cross-linked tetragonal lysozyme crystals and mother liquor solution or the solution with a same composition as mother liquor. For experimental details see Figures 5 and 6.

aldehyde groups would react with protein and the other would stay free in a pore, this free aldehyde group might react with fluorescein, resulting in an increase of the fluorescein adsorbed on the crystal. Experiments that we performed showed no shift in adsorption spectra (Klonis et al., 1998), indicating the absence of reaction between fluorescein and glutaraldehyde.

2) Pores of the native crystals are filled with mother liquor and their adsorption sites are screened by high salt concentrations. Conversely, in the pores of the cross-linked crystals, free ions will be present at relatively low concentrations as the result of intensive washing prior to crystal use, potentially resulting in higher fluorescein distribution coefficients for cross-linked than for native crystals. However, considering that pores occupied maximally 2% of the total liquid volume, this effect is probably insignificant after equilibration.

3) Lysozyme and fluorescein are hydrophobic molecules. Cho and Rhee (1993) showed that immobilization of lipase (EC 3.1.1.3) on alkylamine carrier by cross-linking with glutaraldehyde increased the lipase's hydrophobicity by almost two orders of magnitude. Furthermore, Ibrahim et al. (1994) showed that lysozyme hydrophobicity is increased after the treatment with perillaldehyde. However, direct (experimental) proof cannot be provided due to the lack of an unambiguous experimental procedures for determination of protein hydrophobicity. The influence of the hydrophobicity of solute and protein on the solute uptake by protein crystals will be the subject of future studies.

CONCLUSIONS

Adsorption of fluorescein by lysozyme crystals depends on the characteristics of the fluorescein solution and lysozyme crystal. The affinity of lysozyme crystals for solute increases in the order CHES, MOPS, acetate, and fluorescein. A shift in the adsorption mechanism from noncompetitive to competitive is observed for fluorescein uptake when its solution contains increasing MOPS or CHES concentrations. Adsorption of fluorescein by cross-linked tetragonal lysozyme crystals is exponentially dependent on the lysozyme net charge calculated from the pH of the final solution. A 3–5-fold increase in the fluorescein adsorption occurs as a result of cross-linking, but the adsorption does not seem to depend on the crystal's morphology.

The cross-linked protein crystals may be useful for practical applications, because the observed capacities and affinities are comparable to or better than those of conventional adsorbents. The required process conditions will depend on the specific application, in particular on the solute to be adsorbed.

NOMENCLATURE

a, b, c	unit cell coordinates [m]
b_1	affinity constant of fluorescein for the crystals [L mol^{-1}]
b_2	affinity constant of MOPS for the crystals [L mol^{-1}]
C	concentration [mol L^{-1}]
K	distribution coefficient of fluorescein between crystal and bulk liquid phase
m	mass [kg]
M	molar mass [kg mol^{-1}]
n	number of molecules per unit cell
N_A	Avogadro's number
q	concentration in adsorbed phase [mol kg^{-1}]
Q_{sat}	capacity of the crystals for fluorescein [mol kg^{-1}]
R_L	separation factor
V	volume [L]
α, β, γ	angles between coordinates in unit cell [rad]
ρ	density [kg m^{-3}]

Super- and Subscripts

0	at initial conditions
cr	for crystal phase (including pores)
d	of dry crystals
eq	at equilibrium
Fl	of fluorescein
L	for bulk liquid phase
lys	of lysozyme
s	of solvent in the crystal pores
uc	of the unit cell
w	of water tightly bound to lysozyme

References

Bishop WH, Richards FM. 1968. Properties of liquids in small pores. Rates of diffusion of some solutes in cross-linked crystals of beta-lactoglobulin. J Mol Biol 38:315–328.

Botin AS, Morozov VN. 1985. Transfer of the low molecular weight compounds in protein crystals and films. Biofizika 32:22–28.

Cho SW, Rhee JS. 1993. Immobilization of lipase for effective interesterification of fats and oils in organic-solvent. Biotechol Bioeng 41: 204–210.

Colman PM, Matthews BW. 1971. Symmetry, molecular weight and crystallographic data for sweet potato-amylase. J Mol Biol 60:163–168.

Cvetkovic A, Straathof AJJ, Hanlon DN, van der Zwaag S, Krishna R, van der Wielen LAM. 2004. Quantifying anisotropic solute transport in protein crystals using 3-D laser scanning microscopy visualization. Biotechnol Bioeng 86:389–398.

Diehl H, Morchak-Morris N. 1987. Study on fluorescein-V: the absorbance of fluorescein in the ultraviolet, as a function of pH. Talanta 34: 739–741.

Feher G, Kam Z. 1985. Nucleation and growth of protein crystals: General principles and assays. Meth Enzymol 114:78–112.

Gevorkyan SG, Morozov VN. 1983. Dependence of the hydration isotherm of lysozyme on the packing of the molecules in the solid phase. Biofizika 28:1002–1007.

Granick S. 1942. Some properties of crystalline guinea pig hemoglobin. J Gen Physiol 25:571–578.

Hall KR, Eagleton LC, Acrivos A, Vermeule T. 1966. Pore- and solid-diffusion kinetics in fixed-bed adsorption under constant-pattern conditions. Ind Eng Chem Fund 5:212–223.

Ibrahim HR, Hatta H, Fujiki M, Kim M, Yamamoto T. 1994. Enhanced antimicrobial action of lysozyme against Gram-negative and Gram-positive bacteria due to modification with perillaldehyde. J Agr Food Chem 42:1813–1817.

Jansen ML, Straathof AJJ, Van der Wielen LAM, Luyben KCAM, van denTweel WJJ. 1996. Rigorous model for ion exchange equilibria of strong and weak electrolytes. AIChE J 42:1911–1924.

Kachalova GS, Lanina NF, Atanasov BP, Morozov VN, Shljapnikova EA, Morozova TY. 1995. The X-ray-fluorescence study of the ionic content of the lysozyme crystals. Biofizika 40:274–282.

Klonis N, Clayton AHA, Voss EW, Sawyer WH. 1998. Spectral properties of fluorescein in solvent-water mixtures: applications as a probe of hy-

drogen bonding environments in biological systems. Photochem Photobiol 67:500–510.

Kuehner DE, Engmann J, Fergg F, Wernick M, Blanch HW, Prausnitz JM. 1999. Lysozyme net charge and ion binding in concentrated aqueous electrolyte solutions. J Phys Chem B 103:1368–1374.

Lee HM, Kim YW, Baird JK. 2001. Electrophoretic mobility and zeta-potential of lysozyme crystals in aqueous solutions of some 1:1 electrolytes. J Cryst Growth 232:294–300.

Leung AKW, Park MMV, Borhani DW. 1999. An improved method for protein crystal density measurements. J Appl Cryst 32:1006–1009.

Margolin AL, Navia MA. 2001. Protein crystals as novel catalytic materials. Angew Chem Int Ed 40:2205–2222.

Matthews BW. 1968. Solvent content of protein crystals. J Mol Biol 33:491–497.

McRee D. 1999. Practical protein crystallography. San Diego: Academic Press.

Morozov VN, Morozova TY. 1992. Mechanical detection of interaction of small specific ligands with proteins and DNA in cross-linked samples. Anal Bioch 201:68–79.

Morozov VN, Kachalova GS, Evtodienko VU, Lanina NF, Morozova TY. 1995. Permeability of lysozyme tetragonal crystals to water. Eur Biophys J 24:93–98.

Morozova TY, Kachalova GS, Lanina NF, Evtodienko VU, Botin AS, Shlyapnikova EA, Morozov VN. 1996. Ionic conductivity, transference numbers, composition and mobility of ions in cross-linked lysozyme crystals. Biophys Chem 60:1–16.

O'Hara P, Goodwin P, Stoddard BL. 1995. Direct measurement of diffusion rates in enzyme crystals by video absorbance spectroscopy. J Appl Cryst 28:829–834.

Rupley JA. 1969. The comparison of protein structure in the crystal and in solution. In: Timasheff SN, Fasman GD, editors. Structure and stability of biological macromolecules. New York: Marcel Dekker. p 291–352.

Sjoback R, Nygren J, Kubista M. 1995. Absorption and fluorescence properties of fluorescein. Spectrochim Acta A 51:L7–L21.

Squire PG, Himmel ME. 1979. Hydrodynamics and protein hydration. Arch Biochem Biophys 196:165–177.

St Clair NL, Navia MA. 1992. Cross-linked enzyme crystals as robust biocatalysts. J Am Chem Soc 114:7314–7316.

Steinrauf LK. 1959. Preliminary X-ray data for some new crystalline forms of B-lactoglobulin and hen egg-white lysozyme. Acta Cryst 12: 77–79.

Velev OD, Kaler EW, Lenhoff AM. 2000. Surfactant diffusion into lysozyme crystal matrices investigated by quantitative fluorescence microscopy. J Phys Chem B 104:9267–9275.

Vilenchik LZ, Griffith JP, St Clair N, Navia MA, Margolin AL. 1998. Protein crystals as novel microporous materials. J Am Chem Soc 120:4290–4294.

Walt DR, Agayn VI. 1994. The chemistry of enzyme and protein immobilization with glutaraldehyde. Trends Anal Chem 13:425–430.

Yonath A, Sielecki A, Moult J, Podjarny A, Traub W. 1977. Crystallographic studies of protein denaturation and renaturation. 1. Effect of denaturation on volume and x-ray pattern cross-linked triclinic lysozyme crystals. Biochemistry 16:1413–1417.